



LAWRENCE  
LIVERMORE  
NATIONAL  
LABORATORY

UCRL-TR-235921

# Characterization of BMS-8-212 for use in penetration simulations

G. Kay, D. Urabe, A. Shields, S. DeTeresa

October 29, 2007

## **Disclaimer**

---

This document was prepared as an account of work sponsored by an agency of the United States government. Neither the United States government nor Lawrence Livermore National Security, LLC, nor any of their employees makes any warranty, expressed or implied, or assumes any legal liability or responsibility for the accuracy, completeness, or usefulness of any information, apparatus, product, or process disclosed, or represents that its use would not infringe privately owned rights. Reference herein to any specific commercial product, process, or service by trade name, trademark, manufacturer, or otherwise does not necessarily constitute or imply its endorsement, recommendation, or favoring by the United States government or Lawrence Livermore National Security, LLC. The views and opinions of authors expressed herein do not necessarily state or reflect those of the United States government or Lawrence Livermore National Security, LLC, and shall not be used for advertising or product endorsement purposes.

This work performed under the auspices of the U.S. Department of Energy by Lawrence Livermore National Laboratory under Contract DE-AC52-07NA27344.

## **Characterization of BMS-8-212 for use in penetration simulations**

Gregory Kay  
David Urabe  
Albert Shields  
Steve DeTeresa

Lawrence Livermore National Laboratory  
Livermore, CA 94551

### **Abstract**

BMS 8-212 lamina properties for use in the computational modeling of aircraft shielding systems were determined in this study. The carbon-reinforced BMS 8-212 composite lay-ups that were tested were unidirectional 0.351" thick (45 ply) flat panels. The mechanical responses of the flat panel unidirectional specimens were assumed to be representative of the behavior of the matrix dominated compressive BMS 8-212 lamina responses in the transverse and normal directions. The rate sensitivity of the flat panel specimens was determined for loading rates between  $0.001 \text{ s}^{-1}$  and  $1000 \text{ s}^{-1}$ . In that regime, the transverse and normal failure stresses were found to increase by approximately 1.5.

### **Introduction**

A program to simulate the performance of aircraft composite ballistic shields has been initiated and supported by the Federal Aviation Administration (FAA). Computational constitutive models of the shields are an important part of that program. An important initial step in the FAA program was the determination of the lamina properties of a representation carbon-fiber composite panel. BMS 8-212, grade 190, type 3 class 1 (as classified by Boeing and made by Hexel) was chosen for this study. This material is representative of generic composite panels that could be employed in aircraft shielding systems. This report describes the determination of constitutive properties for a unidirectional 0.351" thick (45 ply) flat panel, and also gives results for a quasi-isotropic 0.361" thick (46 lamina) flat panel laminate that could be of use in later modeling efforts.

In the determination of the BMS 8-212 lamina properties it was assumed that the carbon fibers were essentially rate insensitive and brittle in their stress-strain responses. It was further assumed that the tensile and compressive strengths of the lamina in the longitudinal direction were available in the open literature. Furthermore the elastic properties for the lamina material in all directions were also assumed to be available in the open literature. The matrix dominated compressive properties of the BMS 8-212 were determined by tests employing cylindrical specimens of approximately 0.2745" diameter. These unidirectional lay-up specimens, cored out normal to the BMS 8-212 panels, were assumed to be representative of the matrix dominated compressive lamina BMS 8-212 responses. The rate sensitivity of the BMS 8-212 specimens were determined for loading rates between  $0.001 \text{ s}^{-1}$  and  $1000 \text{ s}^{-1}$ . A description of the tests and the results are given in

Appendix A and a sample input for LSDYNA constitutive model  
“\*MAT\_COMPOSITE\_FAILURE\_MODEL” is given in Appendix B.

## Test Results

Results of the tests for the unidirectional BMS 8-212 lay-up are shown in Figures 1. The results are consistent between the two testing regimes that were considered in the LLNL tests. Those two strain rate regimes were the  $0.001 \text{ s}^{-1}$  to  $10 \text{ s}^{-1}$  regime (performed on a Centorr universal test machine) and the  $1000 \text{ s}^{-1}$  strain rate regime (performed on a split-Hopkinson Bar test machine). Each point on Figure 1 is the average five separate tests. A least squares fit to the unidirectional compressive test data is also given in Figure 1.

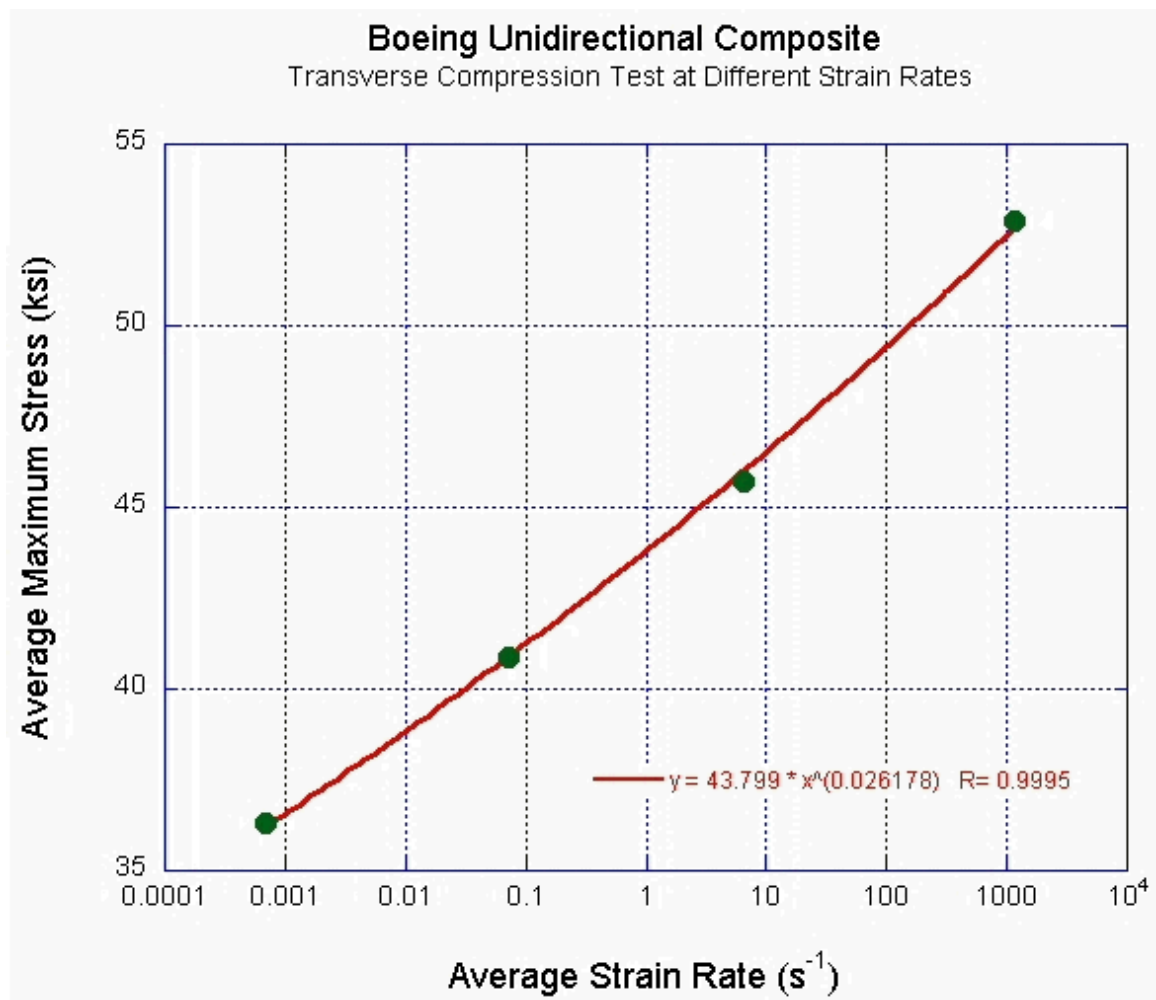


Figure 1. Unidirectional Lay-Up Results for the matrix dominated compressive BMS 2-812 transverse and normal responses.

Results of the tests for the quasi-isotropic 0.361" thick (46 ply) flat panel laminate are summarized in Figure 2. Each point on Figure 2 is the average five separate tests. While these results were not used in the determination of BMS 8-212 lamina properties, they are presented here to provide information about possible future carbon-fiber composite characterization tests. The quasi-isotropic results are not consistent between the  $.001 \text{ s}^{-1}$  to  $10 \text{ s}^{-1}$  (Centorr universal test machine) and  $1000 \text{ s}^{-1}$  strain rate (split Hopkinson Bar) regimes. In fact the maximum stress drops considerably between the two regimes. A possible explanation for the quasi-isotropic material maximum stress drop off at the higher loading rate is that a new laminate failure mechanism is being activated, one that did not come into play for the higher loading rate unidirectional lay-up results

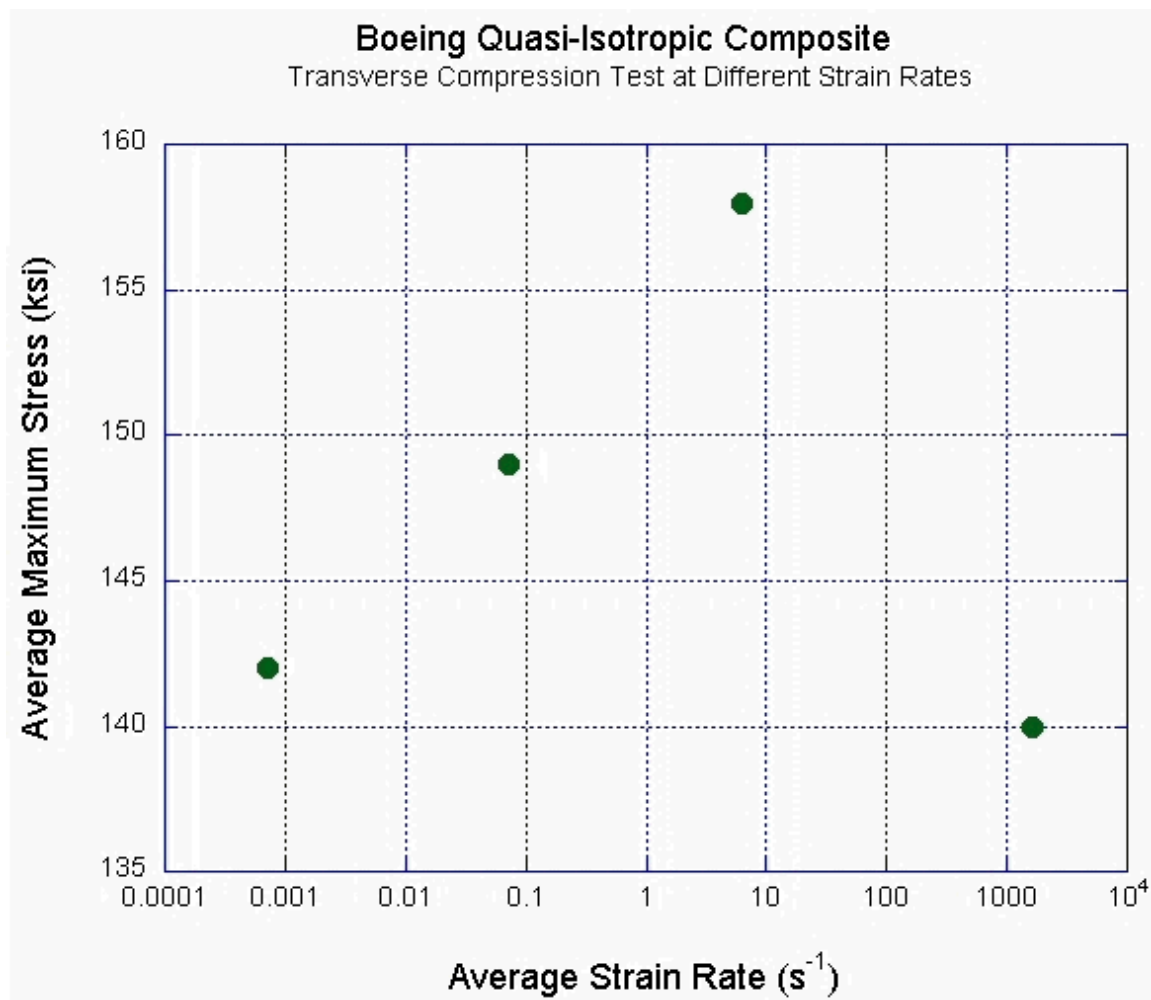


Figure 2. Quasi-Transverse Lay-up Results

### Summary

The compressive transverse and normal failure stresses of the BMS 8-212 lamina material were found to increase according to the following expression for loading rates between  $0.001 \text{ s}^{-1}$  and  $1000 \text{ s}^{-1}$ :

$$R_f = 1.20535 * (\dot{\epsilon})^{0.026178}$$

where  $\dot{\epsilon}$ , the loading direction strain rate, could be represented in a constitutive model by the effective strain rate.

## **Appendix A: Testing description memo from David Urabe to Greg Kay**

June 26, 2007

To: Greg Kay

From: David Urabe

Subject: Formal Report on ETR M0501053 - Boeing Composites

---

### **Test Request**

The request was to formalize the documentation of the work done under ETR M0501053 – Boeing Composites. This report details the work performed by Albert Shields and David Urabe under the direction of Steve DeTeresa during late 2004 and early 2005.

### **Scope**

The work consisted of several tests at different strain rates for Boeing composite material identified as  $0^\circ$  and  $45^\circ$ . The overall details of testing are given in Table 1: Scope of Testing.

### **Test Procedures**

The lower strain rate tests,  $.001 \text{ s}^{-1}$  through  $10 \text{ s}^{-1}$ , were performed using a sub-press assembly for compression with an extensometer to measure displacement on the Centorr universal test machine<sup>1</sup> (See Figure 1) and the higher strain rate tests,  $>1000 \text{ s}^{-1}$ , were done in the split Hopkinson Bar assembly (See Figure 2).

---

<sup>1</sup> Centorr, calibrated on 11/5/2004, ASTM E4

The lower strain rate specimens were measured and the dimensions recorded (See Table 2). Prior to test, the appropriate displacement rates were approximated by multiplying the desired strain rate by the specimen height to obtain an actuator speed for the lower strain rate tests. These values were used for test and compared with actual strain rate values after test. The force, displacement, and time were recorded during test. These and used to calculate stress, strain, and strain rate after test.

The higher strain rate specimens were measured and the dimensions recorded (See Table 3). The test parameters were calculated based on the estimated flow stress of the materials; 40 ksi for 0° and 150 ksi for 45°. The test uses a cylindrical projectile to impact a cylindrical incident bar which has been instrumented with strain gages. The impact sends a compressive stress wave down the incident bar, into the test sample and out through a transmitter bar with similar instrumentation. The signals from the two sets of instrumentation are compared and the net change is used to calculate the stress and strain caused by the stress wave. The strain signals from the two bars during test were captured with an Nicolet Integra system at a rate 5 MHz and evaluated using the KaleidaGraph spreadsheet software to produce graphical representations of stress and strain. These tests were performed at a projectile velocity which would bracket a strain rate of  $1000 \text{ s}^{-1}$  or greater using a 13 inch projectile in our 0.560 inch diameter high strength steel split Hopkinson Bar compression assembly.

## **Test Results**

The lower strain rate test results are tabulated in Table 2: Lower Strain Rate Summary. The test series are compiled for the different materials by strain rate test in figures 3 through 8 with comparison graphs of the two materials by strain rate in figures 9 through 11.

The higher strain rate test results are tabulated in Table 3: Split Hopkinson Bar Summary. The test series are compiled by material, 0° and 45°, in figures 12 and 13 with a comparison graph of the two materials in figure 14.

## **Observations**

There appears to be a small increase in the maximum stress as the strain rate increases for both materials up to the high strain rate of greater than  $1000 \text{ s}^{-1}$  in the Hopkinson bar tests where the 0° material continues to increase, but the 45° begins to show a decrease. However, this may be part of the statistical variation within the composite properties at the higher strain rates. There were no other supporting references for the Boeing material properties.

The Hopkinson bar testing demonstrated the brittle nature of both materials. There was very little flow prior to fracture in all of the tests which showed in the large decrease in strain rate as shown in Table 3. The remnants of a 0° specimen and a 45° specimen after test are shown in Figures 15 and 16, respectively.

| Material ID | Test Strain Rate ( $s^{-1}$ ) | Number of specimens | Specimen IDs       |
|-------------|-------------------------------|---------------------|--------------------|
| 0°          | 0.001                         | 5                   | 1, 2, 3, 4, 5      |
| 0°          | 0.1                           | 5                   | 6, 7, 8, 9, 10     |
| 0°          | 10                            | 5                   | 11, 12, 13, 14, 15 |
| 0°          | >1000                         | 5                   | 16, 17, 19, 20, 21 |
| 45°         | 0.001                         | 5                   | 1, 2, 3, 4, 5      |
| 45°         | 0.1                           | 5                   | 6, 7, 8, 9, 10     |
| 45°         | 10                            | 5                   | 11, 12, 13, 14, 15 |
| 45°         | >1000                         | 5                   | 16, 17, 18, 19, 20 |

**Table 1: Scope of Testing**

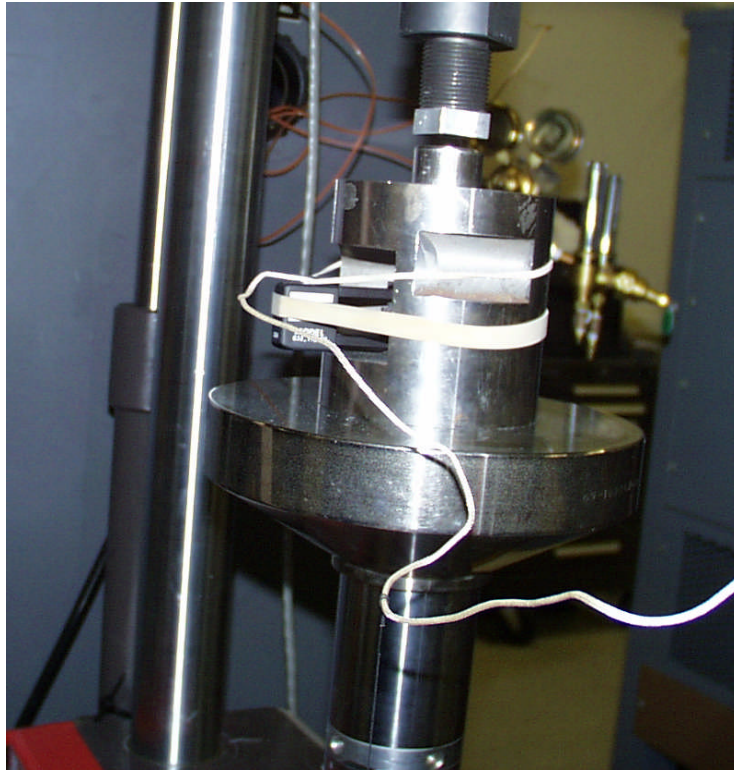


**Figure 1: Sub-press Assembly in Centorr Universal Test Machine**





**Figure 2: Split Hopkinson Bar Compression Assembly**

| Material ID – Specimen ID | Test Strain Rate ( $s^{-1}$ ) | Actual Strain Rate ( $s^{-1}$ ) | Dia. (in) | Height (in) | Weight (gm) | Max. Stress (ksi) | Strain @ Max. Stress (%) | Strain @ Failure Stress (%) |
|---------------------------|-------------------------------|---------------------------------|-----------|-------------|-------------|-------------------|--------------------------|-----------------------------|
| 0° - 1                    | 0.001                         | 0.000351                        | 0.2743    | 0.3504      | 0.5112      | 37.5              | 4.5                      | 4.7                         |
| 0° - 2                    | 0.001                         | 0.000351                        | 0.2745    | 0.3503      | 0.5134      | 35.2              | 4.2                      | 4.3                         |
| 0° - 3                    | 0.001                         | 0.000350                        | 0.2744    | 0.3501      | 0.5149      | 38.4              | 4.2                      | 4.4                         |
| 0° - 4                    | 0.001                         | 0.000351                        | 0.2745    | 0.3502      | 0.5173      | 34.7              | 3.2                      | 3.3                         |
| 0° - 5                    | 0.001                         | 0.000350                        | 0.2744    | 0.3504      | 0.5123      | 35.7              | 4.1                      | 4.4                         |
| 0° - 6                    | 0.1                           | 0.0352                          | 0.2745    | 0.3508      | 0.5186      | 41.2              | 4.1                      | 4.2                         |
| 0° - 7                    | 0.1                           | 0.0352                          | 0.2744    | 0.3504      | 0.5132      | 41.6              | 4.5                      | 4.6                         |
| 0° - 8                    | 0.1                           | 0.0352                          | 0.2744    | 0.3504      | 0.5127      | 41.8              | 4.6                      | 4.7                         |
| 0° - 9                    | 0.1                           | 0.0352                          | 0.2742    | 0.3501      | 0.5097      | 39.5              | 4.5                      | 4.5                         |
| 0° - 10                   | 0.1                           | 0.0352                          | 0.2746    | 0.3503      | 0.5200      | 40.6              | 4.0                      | 4.0                         |
| 0° - 11                   | 10                            | 3.02                            | 0.2745    | 0.3504      | 0.5120      | 45.2              | 4.4                      | 4.4                         |

|          |       |              |        |        |        |      |      |      |
|----------|-------|--------------|--------|--------|--------|------|------|------|
| 0° - 12  | 10    | 2.99         | 0.2742 | 0.3502 | 0.5101 | 44.3 | 4.3  | 4.3  |
| 0° - 13  | 10    | 2.99         | 0.2744 | 0.3501 | 0.5096 | 45.9 | 4.5  | 4.5  |
| 0° - 14  | 10    | 2.97         | 0.2745 | 0.3503 | 0.5151 | 46.8 | 4.8  | 5.5  |
| 0° - 15  | 10    | 2.99         | 0.2745 | 0.3504 | 0.5174 | 46.2 | 4.6  | 5.2  |
| 45° - 1  | 0.001 | 0.00036<br>0 | 0.2745 | 0.3604 | 0.5281 | 146  | 10.3 | 10.3 |
| 45° - 2  | 0.001 | 0.00036<br>0 | 0.2745 | 0.3609 | 0.5286 | 140  | 10.2 | 10.2 |
| 45° - 3  | 0.001 | 0.00036<br>0 | 0.2744 | 0.3614 | 0.5277 | 148  | 11.1 | 11.1 |
| 45° - 4  | 0.001 | 0.00036<br>0 | 0.2743 | 0.3611 | 0.5283 | 144  | 10.0 | 10.0 |
| 45° - 5  | 0.001 | 0.00036<br>0 | 0.2746 | 0.3613 | 0.5277 | 130  | 9.4  | 9.4  |
| 45° - 6  | 0.1   | 0.0360       | 0.2750 | 0.3613 | 0.5307 | 151  | 10.7 | 10.7 |
| 45° - 7  | 0.1   | 0.0361       | 0.2749 | 0.3615 | 0.5298 | 150  | 10.2 | 10.2 |
| 45° - 8  | 0.1   | 0.0362       | 0.2743 | 0.3611 | 0.5272 | 150  | 10.3 | 10.3 |
| 45° - 9  | 0.1   | 0.0361       | 0.2748 | 0.3612 | 0.5304 | 149  | 10.5 | 10.5 |
| 45° - 10 | 0.1   | 0.0361       | 0.2744 | 0.3610 | 0.5277 | 145  | 9.9  | 9.9  |
| 45° - 11 | 10    | 3.04         | 0.2744 | 0.3611 | 0.5284 | 167  | 11.1 | 11.8 |
| 45° - 12 | 10    | 3.04         | 0.2745 | 0.3619 | 0.5289 | 155  | 10.7 | 10.8 |
| 45° - 13 | 10    | 3.03         | 0.2746 | 0.3605 | 0.5262 | 149  | 10.1 | 10.1 |
| 45° - 14 | 10    | 3.03         | 0.2745 | 0.3615 | 0.5297 | 164  | 11.2 | 11.2 |
| 45° - 15 | 10    | 3.03         | 0.2744 | 0.3601 | 0.5278 | 154  | 10.2 | 10.2 |

**Table 2: Lower Strain Rate Summary**

| Material ID<br>-<br>Specimen ID | Height<br>(in) | Dia.<br>(in) | Weight<br>(gm) | Strain rate<br>(s <sup>-1</sup> )<br>max - min | Maximum<br>Stress<br>(ksi) | Engineering<br>Strain<br>(%) |
|---------------------------------|----------------|--------------|----------------|--|----------------------------|------------------------------|
| 0° - 16                         | 0.3503         | 0.2744       | 0.5144         | 1730-980                                       | 53.3                       | 5.2                          |
| 0° - 17                         | 0.3503         | 0.2742       | 0.5141         | 1830-1010                                      | 54.9                       | 5.6                          |
| 0° - 19                         | 0.3503         | 0.2743       | 0.5101         | 1680-990                                       | 51.5                       | 5.1                          |
| 0° - 20                         | 0.3502         | 0.2744       | 0.5168         | 1650-970                                       | 54.0                       | 5.4                          |
| 0° - 21                         | 0.3504         | 0.2746       | 0.5175         | 1700-880                                       | 51.0                       | 4.9                          |
| 45° - 16                        | 0.3614         | 0.2744       | 0.5282         | 2610-900                                       | 146                        | 11                           |
| 45° - 17                        | 0.3614         | 0.2750       | 0.5297         | 2460-880                                       | 139                        | 13                           |
| 45° - 18                        | 0.3615         | 0.2750       | 0.5305         | 2510-900                                       | 150                        | 11                           |
| 45° - 19                        | 0.3615         | 0.2745       | 0.5291         | 2720-1020                                      | 134                        | 10                           |
| 45° - 20                        | 0.3607         | 0.2742       | 0.5278         | 2780-1130                                      | 132                        | 10                           |

**Table 3: Split Hopkinson Bar Summary**

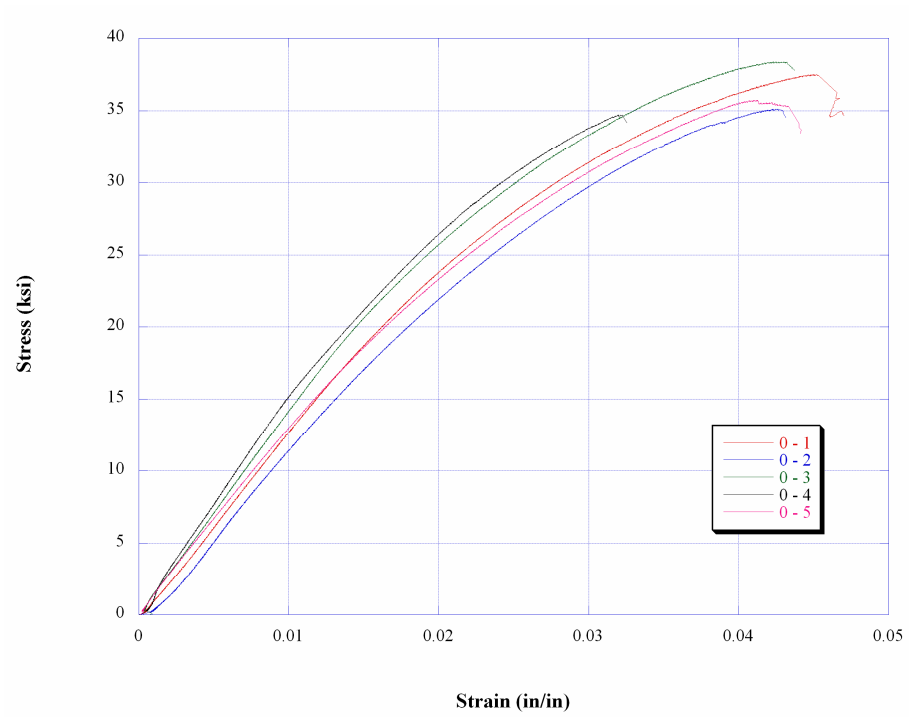


**Figure 3: Boeing 0° at Test Strain Rate of 0.001s<sup>-1</sup>**

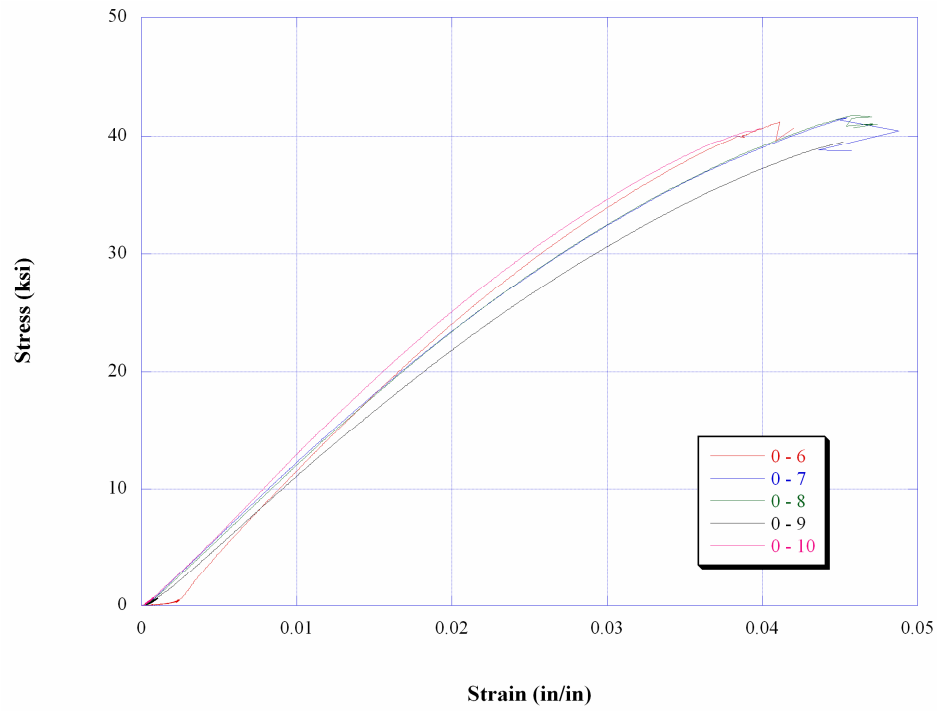


**Figure 4: Boeing 0° at Test Strain Rate of 0.1s<sup>-1</sup>**

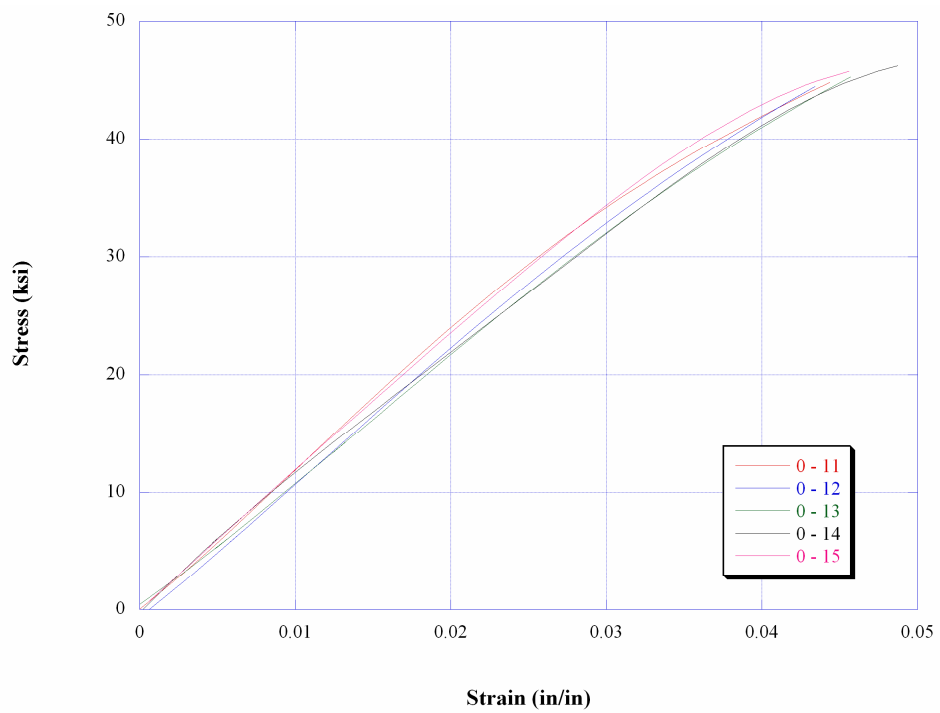


**Figure 5: Boeing 0° at Test Strain Rate of 10s<sup>-1</sup>**

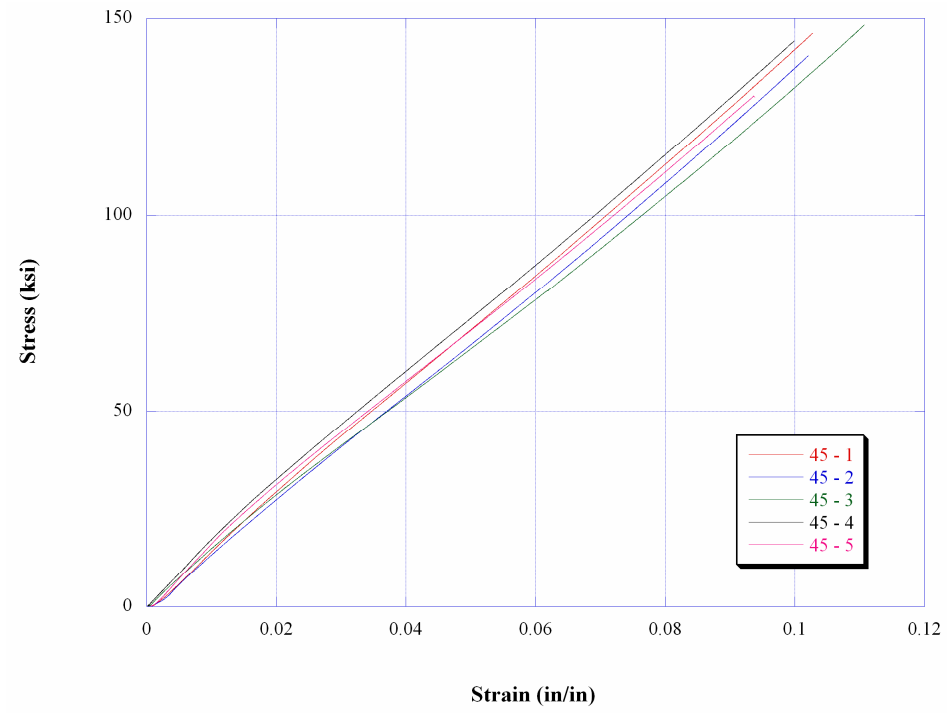


**Figure 6: Boeing 45° at Test Strain Rate of  $0.001\text{s}^{-1}$**

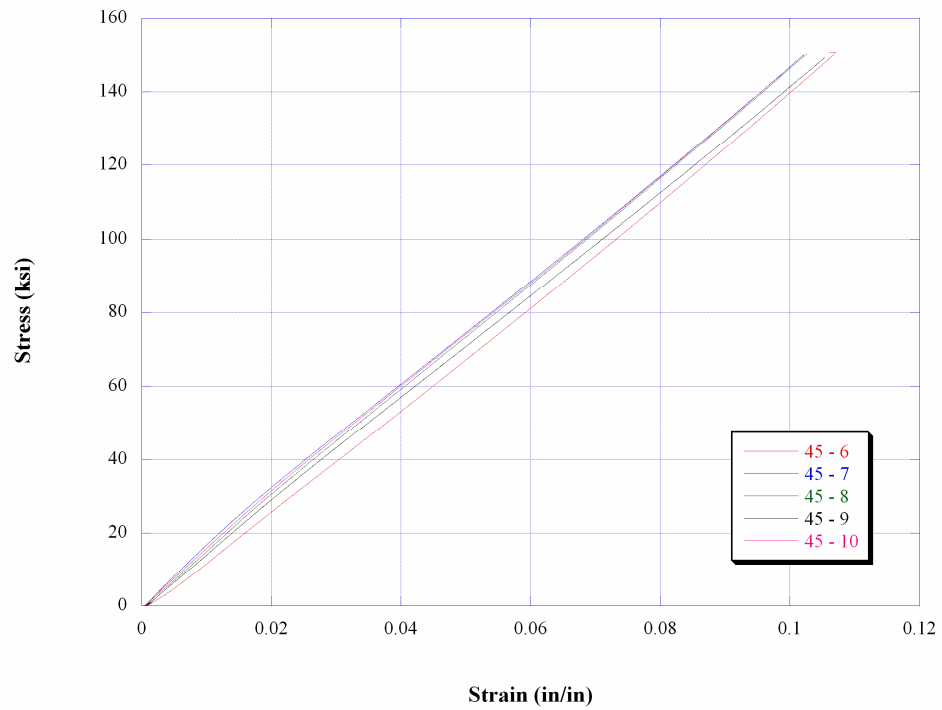


**Figure 7: Boeing 45° at Test Strain Rate of  $0.1\text{s}^{-1}$**

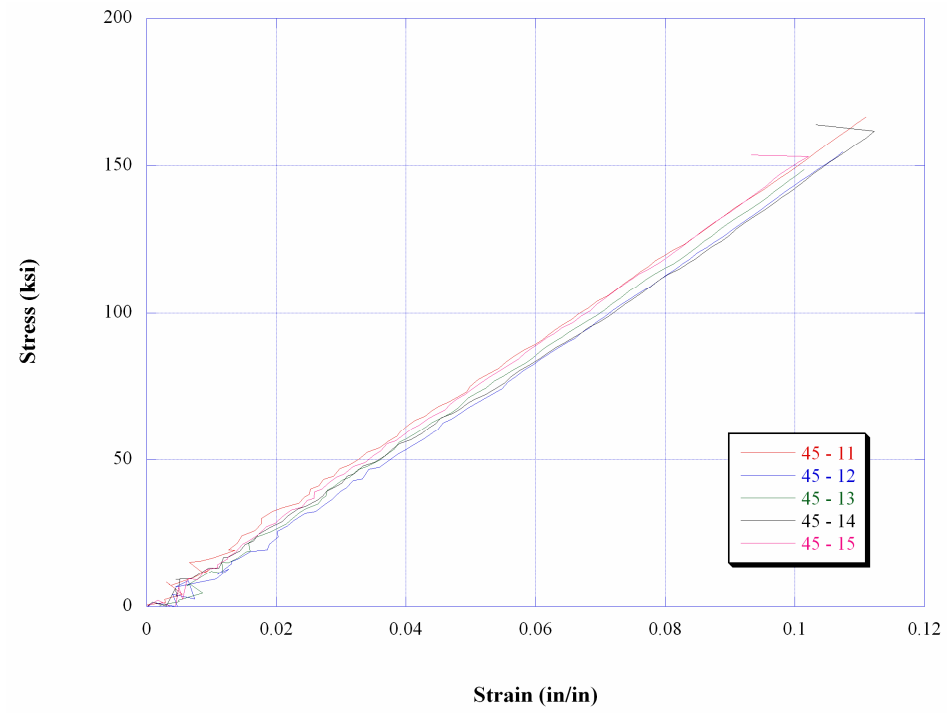


**Figure 8: Boeing 45° at Test Strain Rate of  $10\text{s}^{-1}$**

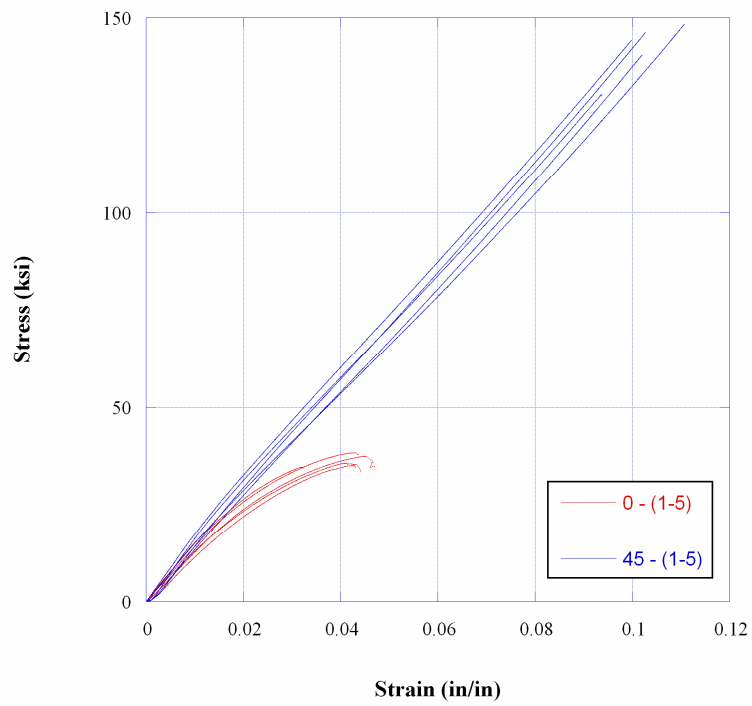


**Figure 9: Boeing 0° and 45° at Test Strain Rate of 0.001s<sup>-1</sup>**

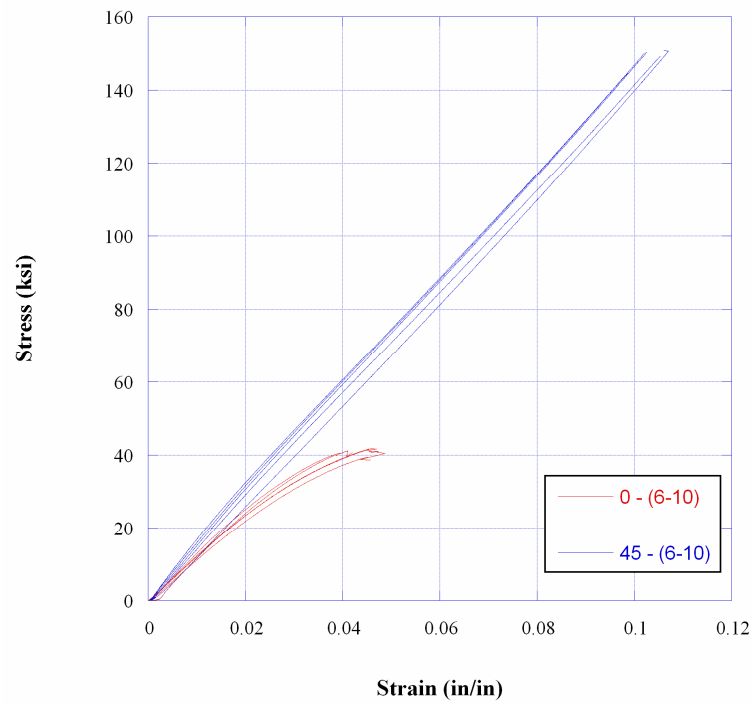


**Figure 10: Boeing 0° and 45° at Test Strain Rate of 0.1s<sup>-1</sup>**

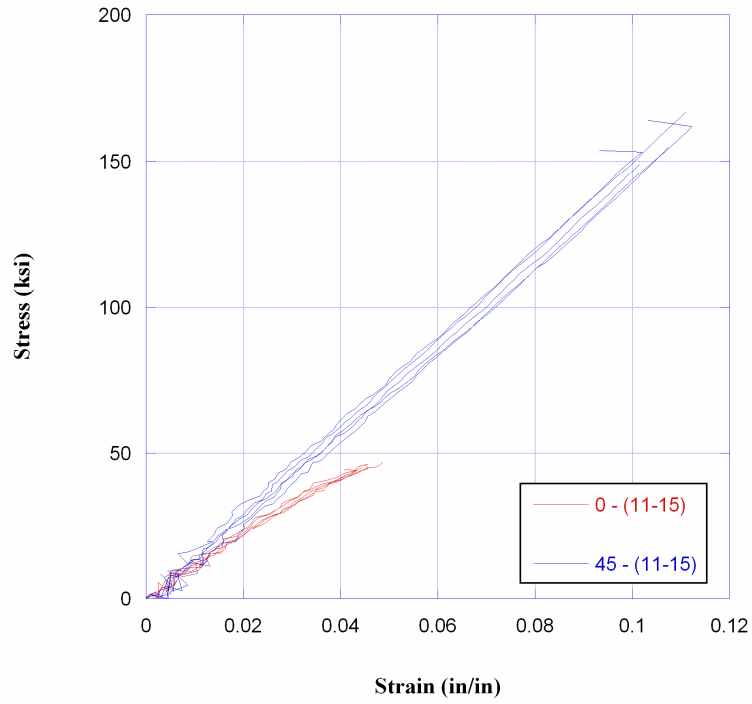


**Figure 11: Boeing 0° and 45° at Test Strain Rate of  $10s^{-1}$**

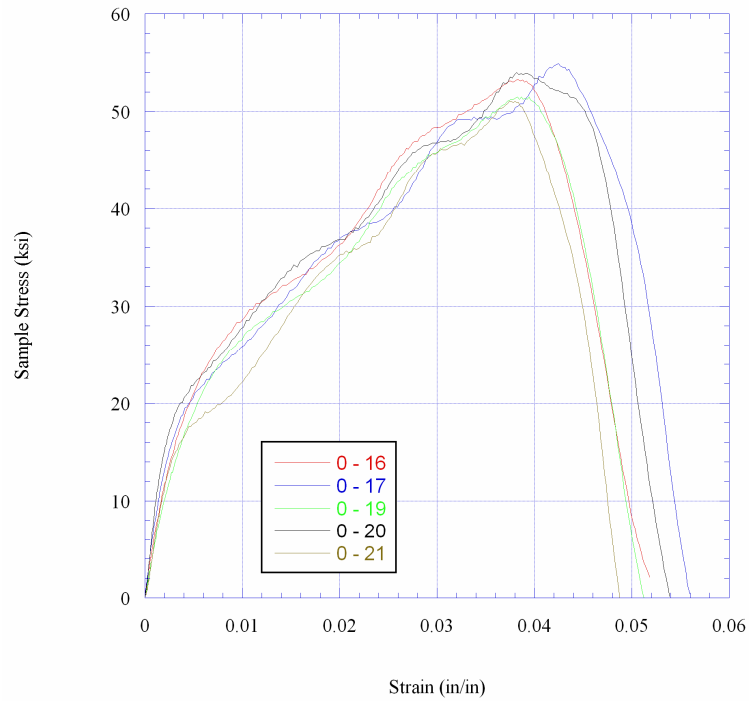


**Figure 12: Boeing 0° at Test Strain Rates greater than  $1000s^{-1}$**



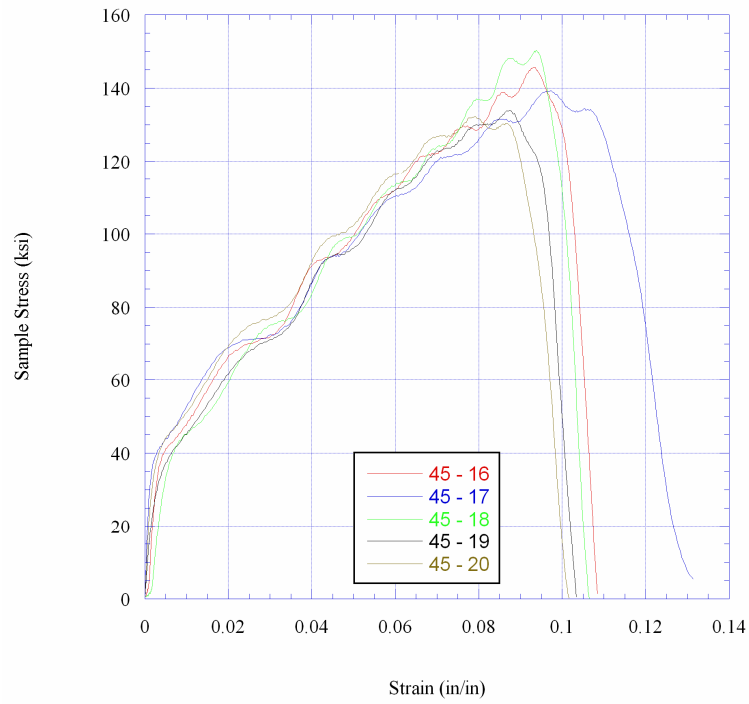


**Figure 13: Boeing 45° at Test Strain Rates greater than  $1000\text{s}^{-1}$**

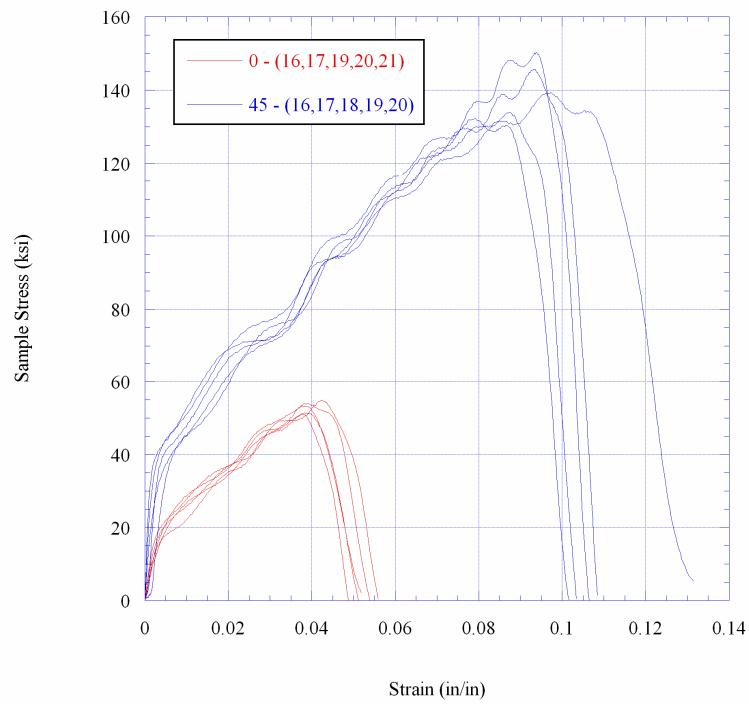


**Figure 14: Boeing 0° and 45° at Test Strain Rates greater than  $1000\text{s}^{-1}$**

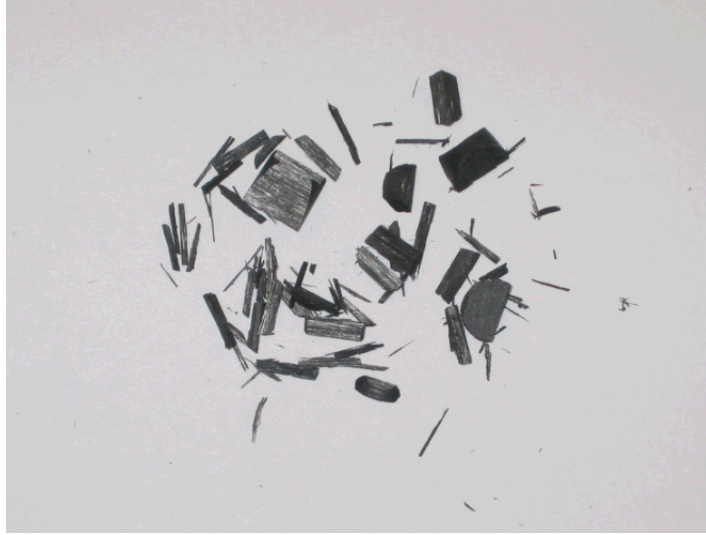


**Figure 15: Boeing 0° Typical Specimen post Hopkinson Bar Test**



**Figure 16: Boeing 45° Typical Specimen post Hopkinson Bar Test**

If there are any questions about the results of this work, please contact me.

---

David Urabe  
Materials Engineering Group

Reviewer Initials: TA

Authors Initials: DU

Electronic CC:

T. Andrews

**Appendix B: BMS 2-812 input for LSDYNA constitutive model**  
**“\*MAT\_COMPOSITE\_FAILURE\_MODEL”**

The lamina (ply) properties for BMS-2-812 given in the following table are for use in a constitutive model that assumed an orthotropic elastic *averaged* behavior for each element. For a multi-angle composite, this would imply pre-processing of the plies contained in each element to produce the required averaged behavior input for the constitutive model. Alternatively, if the thickness of each element in a mesh represented a single ply of a laminate material then lamina properties could be used as the constitutive model input. These restrictions were not assumed to apply in the case of a unidirectional laminate, i.e., the unidirectional lamina properties were assumed to be applicable to elements that contained many ply layers.

The elastic properties and fiber direction strengths listed below are from Boeing and from communications with Steve DeTeresa. The matrix dominated compressive strengths were measured at LLNL and the tensile matrix properties were estimated. For the unidirectional lamina the A direction is the fiber direction, X is the fiber direction strength, B is the transverse direction (Y is the transverse strength) and C is the normal direction (Z is the normal direction strength). The fiber direction strengths were assumed to be rate insensitive. The strength enhancement factor for the matrix dominated compressive strengths was determined to be:

$$R_f = 1.20535 * (\dot{\epsilon})^{0.026178}$$

Table. BMS 8-212 input for LSDYNA material model  
 “\*MAT\_COMPOSITE\_FAILURE\_MODEL”

|                 |                         |  |
|-----------------|-------------------------|--|
| Density         | $1.4493 \times 10^{-4}$ | lbf-sec <sup>2</sup> /in <sup>4</sup>                                |
| E <sub>a</sub>  | $1.71 \times 10^7$ psi  | Young's modulus in the longitudinal direction                        |
| E <sub>b</sub>  | $1.28 \times 10^6$ psi  | Young's modulus in the transverse direction                          |
| E <sub>c</sub>  | $1.28 \times 10^6$ psi  | Young's modulus in the normal direction                              |
| v <sub>ba</sub> | 0.02545                 | Poisson's ratio  |
| v <sub>ca</sub> | 0.02545                 | Poisson's ratio  |
| v <sub>cb</sub> | 0.30000                 | Poisson's ratio  |
| G <sub>ab</sub> | $0.800 \times 10^6$ psi | Shear modulus in the ab plane  |
| G <sub>bc</sub> | $0.367 \times 10^6$ psi | Shear modulus in the bc plane  |
| G <sub>ca</sub> | $0.367 \times 10^6$ psi | Shear modulus in the ca plane  |
| S <sub>ba</sub> | 10,000 psi              | In plane shear strength  |
| S <sub>ca</sub> | 10,000 psi              | Transverse shear strength  |
| S <sub>cb</sub> | 10,000 psi              | Transverse shear strength  |
| XX <sub>c</sub> | $1.5 \times 10^5$ psi   | Longitudinal compressive strength                                    |
| YY <sub>c</sub> | 36,341 psi              | Transverse compressive strength,<br>LLNL testing at zero strain rate |
| ZZ <sub>c</sub> | 36,341 psi              | Normal compressive strength,<br>LLNL testing at zero strain rate     |
| XX <sub>t</sub> | $1.6 \times 10^5$ psi   | Longitudinal tensile strength  |
| YY <sub>t</sub> | 8,000 psi               | Transverse tensile strength  |
| ZZ <sub>t</sub> | 8,000 psi               | Normal tensile strength  |